PROCEEDINGS, 50th Workshop on Geothermal Reservoir Engineering
Stanford University, Stanford, California, February 10-12, 2025
SGP-TR-229

Comprehensive Evaluation of Geothermal Potential at Mount Ciremai Geothermal Field, Indonesia, Using Reservoir Modelling and Uncertainty Quantification Method

Ken Dekkers, Michael Gravatt, Michael O'Sullivan, Bei Nagoro, John O'Sullivan

Department of Engineering Science, University of Auckland, 70 Symonds Street, Grafton, Auckland 1010, New Zealand

afua107@aucklanduni.ac.nz

Keywords: Geothermal Energy, Mount Ciremai Geothermal Field, Numerical Reservoir Modelling, Resource Assessment

ABSTRACT

Evaluating geothermal potential is an essential step in determining the sustainability of a geothermal project, both technically and economically. This study assesses the Mount Ciremai Geothermal Field in Indonesia to determine its feasibility for clean electricity generation through 3D reservoir modelling and numerical simulations. A 3D conceptual model was developed by integrating stratigraphy, lithology, structural alignments, and magneto-telluric data.

A numerical simulation was conducted using AUTOUGH2 and the final calibrated model has a total upflow of 56 kg/s with an enthalpy of 1,250 kJ/kg. The model accurately represented surface features, such as the alignment of hot springs. Resource estimation combined with Approximate Bayesian Computation (ABC), iterative algorithms, and numerical modelling, estimated a low P90 power output of 1.1 MWe for 25 years due to the low water table limiting natural discharge. However, by drilling deviated wells from a 500m lower elevation, the estimated resource potential increased significantly to P90/P50/P10 values of 28.6/37.5/55.1 MWe.

This study emphasizes the importance of reservoir modelling in the geothermal pre-development phase. It demonstrates that well placement and accurate 3G data integration (hydrogeological, geological, geochemical, and geophysical) are crucial for estimating and optimizing the resource potential within the system. The findings provide valuable insights into geothermal reservoir assessment and highlight how adaptive drilling strategies can significantly improve feasibility.

1. INTRODUCTION

Indonesia, situated within the Pacific Ring of Fire, holds significant geothermal energy potential, estimated at 23.7 GW as of 2020. The country is the world's second-largest geothermal energy producer, with 2.4 GW in operation, accounting for 15% of global installed capacity. To further develop this resource, the Government of Indonesia (GOI) aims to expand geothermal capacity by 3.3 GW by 2030. One promising prospect is the Mount Ciremai Geothermal Working Area (WKP) in West Java (**Error! Reference source not found.**), a volcanic-type geothermal system spanning 38,560 hectares.

Preliminary surveys by the Indonesian Geology Agency in 2021 identified surface temperature anomalies and geothermal manifestations in the Mount Ciremai region. While 3G methods form the basis of geothermal exploration, they have limitations, making complementary approaches like natural state simulation essential. The first stage of this method is to set up a digital conceptual model integrating exploration data into a detailed, visual model, improving understanding of subsurface conditions and enhancing the field's appeal to investors. This study evaluates the geothermal potential of Mount Ciremai using natural state modeling and uncertainty quantification, thus supporting Indonesia's 2030 geothermal expansion goals.

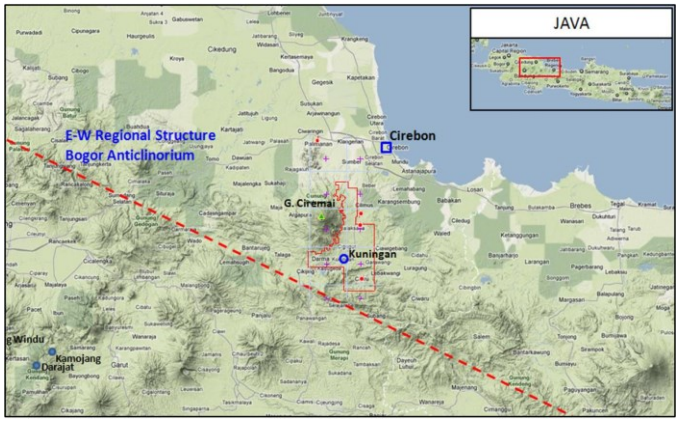

Figure 1: Map of the Mount Ciremai Geothermal Prospect Area

2. GEOLOGICAL SETTINGS OF CIREMAI GEOTHERMAL SYSTEM

The stratigraphy of the Mount Ciremai Geothermal Prospect is defined by geological mapping and literature reviews (Sukaesih et al., 2021; Silitonga et al., 1996; Djuri, 2011). The oldest unit, the Cinambo Formation (TOMC, Tertiary-Oligocene), consists of sandstone and shale uplifted by tectonic activity. Overlying this, the Halang Formation (TMH, Miocene) includes sandstones, mudstones, breccia, and igneous intrusions, deposited in a deep-marine environment. The Ciherang Formation (TPCH, Pliocene) comprises volcaniclastic breccia, tuffaceous sandstone, and conglomerates, formed in terrestrial to transitional settings. The Kaliwangi Formation (TPK, Pliocene) features granitic intrusions, basalts, and rhyolites, reflecting multiple volcanic events with possible marine influences. Younger units include the Cijolang Formation (TPC), with polymictic conglomerates and tuffaceous sandstones, and the Older (QVU) and Younger (QYU) Volcanic Eruption layers, representing successive Mount Ciremai eruptions. The Alluvial Layer (QA) consists of unconsolidated river and floodplain sediments, marking recent geological activity. These units provide a framework for understanding the geothermal potential of Mount Ciremai.

The geological structure of Mount Ciremai is shaped by volcanic and tectonic processes, as shown in Figure 2. The twin-crater system at the summit, covering ~2 km² each, hosts surface geothermal manifestations, including fumaroles releasing heat and gases from the magmatic pathway. The 4.5 km-wide Gegerhalang caldera, a horseshoe-shaped depression, reflects significant past volcanic activity. Fault systems, particularly in the southeastern and southern regions, exhibit elevated fracture density (FFD) along a northwest-southeast trend, that act as conduits for hydrothermal fluids. For example, a fault intersecting a normal fault at the Cilengkrang hot springs allows geothermal waters to reach the surface. These faults, formed during the pre-Quaternary (Pleistocene) period, are validated through LIDAR and geophysical analyses, highlighting their critical role in geothermal fluid circulation within the Mount Ciremai system.

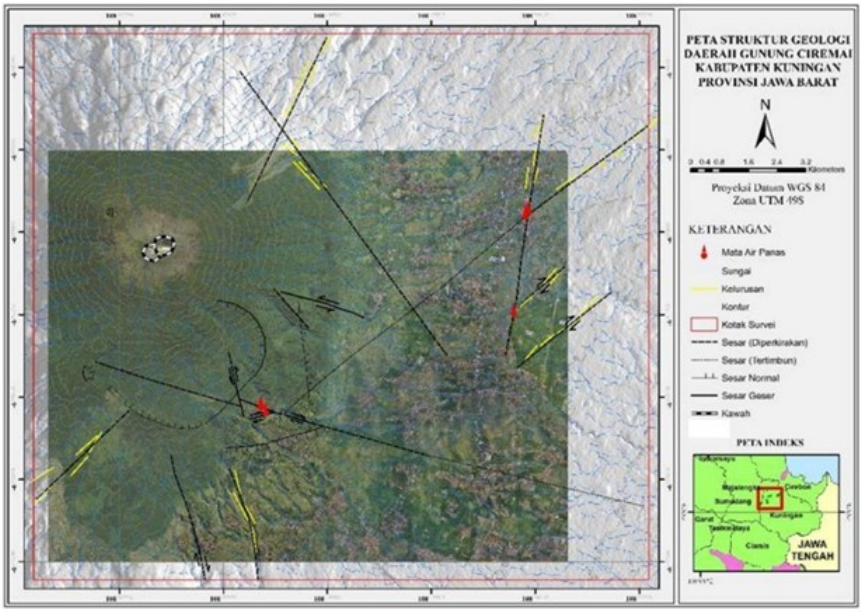

Figure 2: The overlayed figures from LIDAR and Geological Map (Sukaesih et al., 2021)

3. GEOCHEMICAL STUDIES AND ANALYSIS

The geochemical study of the Mount Ciremai Geothermal Field is based on a literature review and is crucial for constructing a conceptual model and numerical natural state model of the geothermal system. Several geothermal surface manifestations are present in Kuningan Regency, West Java, near Mount Ciremai. These include fumaroles at the summit crater and hot springs at Cilengkrang, Sangkanhurip, and Ciniru. Additionally, Subang and Ciangir hot springs, located southeast of Mount Ciremai, were analyzed for comparative purposes. These manifestations provide direct evidence of geothermal activity and help in classifying the geothermal system.

3.1 Cl-SO4-HCO3 Ternary Diagram

Geochemical analysis of Cilengkrang hot springs indicates a chloride-dominated composition, suggesting volcanic influences from Mount Ciremai's magmatic system (**Error! Reference source not found.**). Sangkanhurip and Ciniru hot springs also exhibit chloride dominance, implying geothermal outflow from a deep reservoir. However, Subang and Ciangir hot springs show exceptionally high chloride levels and minimal sulphate/bicarbonate content, indicating a possible seawater influence or interaction with marine sediments.

3.2 Na-K-Mg Ternary Diagram

The Na-K-Mg ternary diagram (**Error! Reference source not found.**) categorizes all geothermal waters from Mount Ciremai as "immature", indicating a significant mixing of geothermal fluids with surface water before reaching equilibrium. Subang hot springs show partial equilibrium, suggesting stronger interaction with reservoir rocks. Meanwhile, Ciangir hot springs plot outside the

equilibrium line, reinforcing the hypothesis that they are influenced by seawater interaction rather than being part of a purely volcanic geothermal system.

3.3 Cl-Li-B Ternary Diagram

The Cl-Li-B ternary diagram (**Error! Reference source not found.**) further distinguishes the geothermal water sources. Cilengkrang, Sangkanhurip, and Ciniru hot springs cluster near the chloride (Cl) apex, confirming a volcanic origin with minor sedimentary influences. Subang hot springs plot along the Cl-B axis, suggesting stronger sedimentary interactions. The Ciangir hot springs, with their high Cl concentration, further validate the seawater influence, reinforcing the idea that Subang and Ciangir belong to separate geothermal systems distinct from Mount Ciremai.

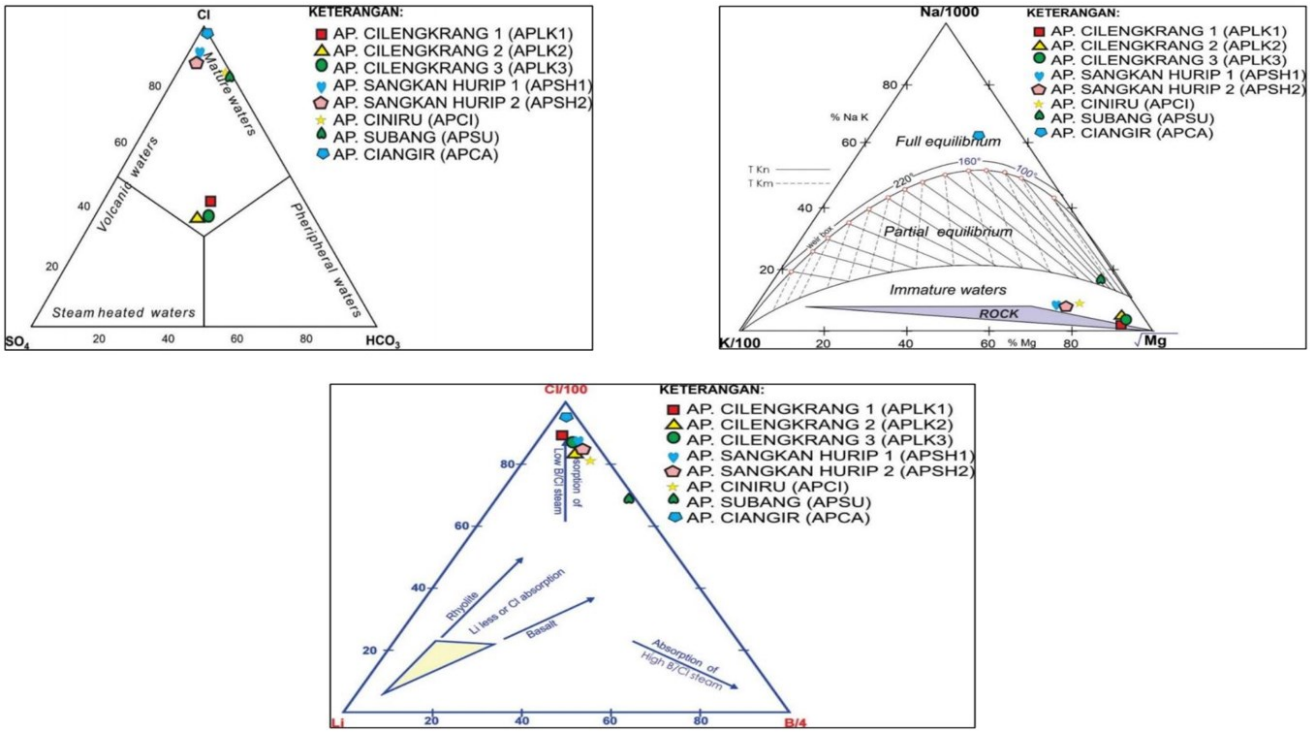

Figure 3: Ternary plots of the Mount Ciremai water sample: (Left – Right – Bottom: Cl-SO4-HCO3, Na-K-Mg, Cl-Li-B) Source: (Kusnadi et al., 2021)

4. GEOPHYSICAL SURVEYS

A structural analysis of Mount Ciremai was conducted using the First Horizontal Derivative (FHD) method, as reported by Dewi, Widodo, and Taryana (2021). High FHD anomalies were identified in the southern region and the eastern part of the summit, connecting the Cilengkrang hot springs to the Ciniru-Sangkan Hurip hot springs. These anomalies suggest the presence of significant geological structures controlling geothermal fluid movement. The FHD map also reveals a boundary between sedimentary and volcanic rocks, marking the location of the Ciniru and Sangkan Hurip hot springs. Additionally, the identification of intersections of structures from the FHD interpretation and LIDAR results confirms the structural control over Cilengkrang hot springs.

A 2.5-dimensional geophysical model was developed using two cross-sections as can be seen in **Error! Reference source not found.**, one trending northwest-southeast (through the summit and Cilengkrang hot springs) and another southwest-northeast (connecting Cilengkrang and Sangkanhurip hot springs). This model revealed the distribution of volcanic and sedimentary rocks, where young volcanic deposits dominate the summit, while older volcanic deposits (Gegerhalang and Sukageri lava intrusions) exist at deeper levels. Beneath these, a sedimentary basement underlies the entire region. Additionally, the model identified a graben structure, step faults, and normal faults, with Cilengkrang hot springs controlled by a normal fault and Sangkanhurip hot springs associated with a shear fault.

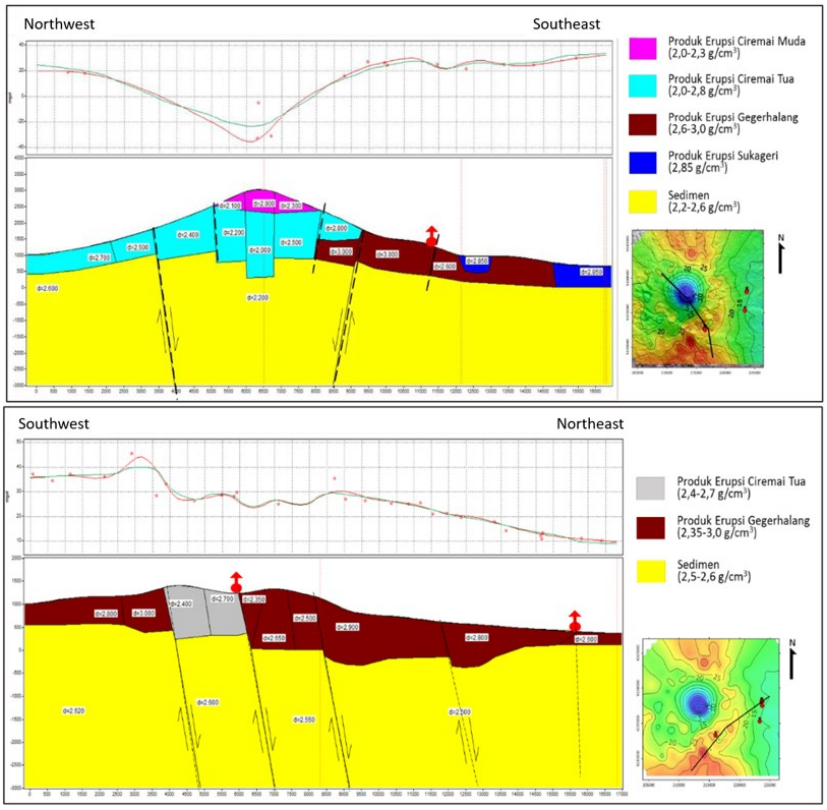

Figure 4: NW-SW (Top) and SW-NE (Bottom) cross-section 2.5D modelling of Mount Ciremai (Dewi et al., 2021)

To enhance the understanding of Mount Ciremai's geothermal system, Magneto-Telluric (MT) and Time-Domain Electromagnetic (TDEM) surveys were integrated with previous MT survey data from 2017 (Takodama et al., 2021). This compiled resistivity model plays a crucial role in delineating prospective geothermal zones and is essential for constructing a conceptual model of the Mount Ciremai geothermal prospect. The resistivity model provides insights into subsurface fluid movement and heat distribution, supporting further exploration and resource assessment. The resistivity survey results indicate a potential geothermal reservoir covering approximately 3 km² near Cilengkrang hot springs, suggesting an upflow zone. This reservoir layer exhibits a moderate resistivity range (20–100 Ohm.m) beneath a low-resistivity overburden layer (<10 Ohm.m). The apex of the reservoir is estimated to be between 1000 m and 1500 m depth, as shown in **Error! Reference source not found.**. These findings provide valuable guidance for future geothermal exploration and development strategies.

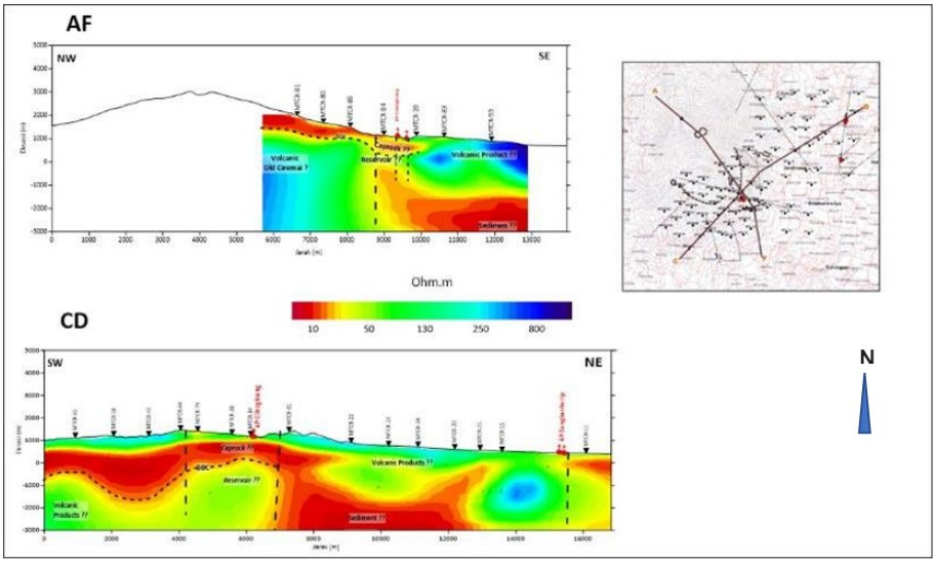

Figure 5: Interpretation result of MT Cross-sections (Takodama et al., 2021)

5. CONCEPTUAL MODEL OF THE CIREMAI GEOTHERMAL FIELD

A geothermal conceptual model describes key geological features and processes governing the system, revealing temperature distribution and fluid flow patterns (Boseley et al., 2010; Cumming, 2009). Using geological, geochemical, geophysical, and hydrogeological data, we developed a conceptual model for the Mount Ciremai geothermal system, which is influenced by volcanic-magmatic activity and contains moderate-temperature fluids.

Figure 6 presents a plan view of the conceptual model, identifying 14 faults through structural analysis. Faults "D," "H," and "G" act as barriers restricting fluid flow, while faults "X," "B," and "E" serve as conduits, facilitating hydrothermal circulation and influencing temperature distribution. The Cilengkrang hot spring is associated with faults "X" and "B," and fault "E" channels outflow to the Sangkanhurip and Ciniru hot springs.

Furthermore, two cross-sections were generated along faults "E" (A-A') and "B" (B-B'), incorporating details of the clay cap, faults, surface manifestations, and water table. Cross-section A-A' (**Error! Reference source not found.**) shows an upwelling heat source, probably distant from Mount Ciremai's main magmatic pathway, heating reservoir fluids that emerge at the Cilengkrang hot springs (57°C). Geochemical analysis indicates a chloride-dominant composition with balanced sulfate and bicarbonate, suggesting contributions from magmatic sources (Kusnadi et al., 2021). Geothermometer results estimate a reservoir temperature of 200°C, supporting Cilengkrang as the upflow zone.

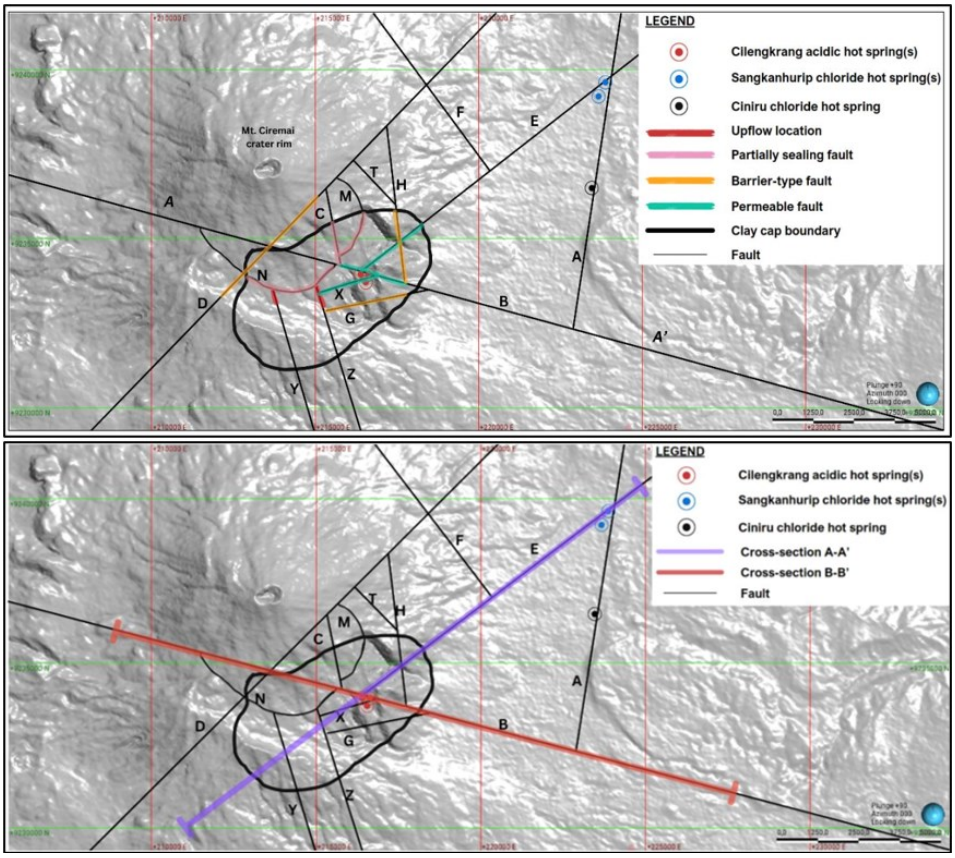

Figure 6: Plan view of Mount Ciremai Geothermal System With Faults (Top) and Corss Section Cuts (Bottom)

Fluid flows eastward along fault "E," creating an outflow that surfaces at the Sangkanhurip and Ciniru hot springs (40-45°C). These springs exhibit nearly pure chloride water with minimal bicarbonate and sulfate, and geothermometer readings indicate a subsurface temperature of ~145°C, confirming this area as the outflow zone.

Cross-section B-B' in **Error! Reference source not found.** visualizes the system along fault "B," showing fluid upwelling toward the clay cap domes and surfacing at Cilengkrang. Fault "E" directs eastward flow to Sangkanhurip and Ciniru, while fault "G" acts as a barrier, confining fluid movement to the southeastern region.

It is important to note that this conceptual model, which identifies Cilengkrang as the upflow zone and Ciniru as the outflow zone, is based on limited data and represents our current interpretation. Additional data may lead to alternative interpretations in the future.

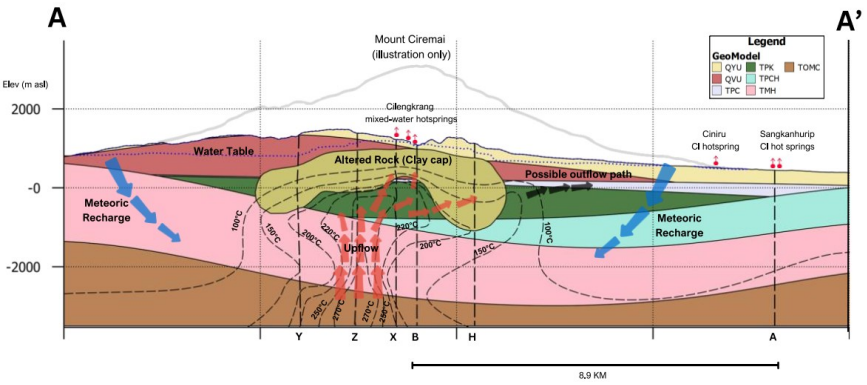

Figure 7: Conceptual Model of Mount Ciremai Geothermal Prospect for A-A' Cross Section

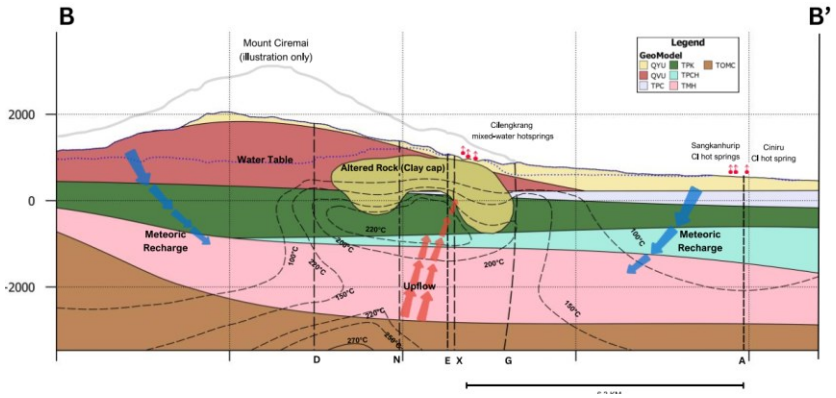

Figure 8: Conceptual Model of Mount Ciremai Geothermal Prospect for B-B' Cross Section

6. STORED HEAT CALCULATION

This study employs the stored-heat (volumetric) method (Grant & Bixley, 2011; Zarrouk & Simiyu, 2013) to estimate the extractable energy potential of the Mount Ciremai geothermal system, providing a baseline for comparison with more complex numerical production models (Glassley, 2010). While the stored-heat method is straightforward, it is subject to uncertainties in parameters such as reservoir size, thickness, and fluid flow dynamics. To address these uncertainties, Monte Carlo simulations (Grant & Bixley, 2011) were applied, assigning probability distributions to key parameters, including reservoir area, depth, porosity, average temperature, recovery factor, and parasitic load. By repeatedly sampling these distributions and integrating them into the stored-heat calculation, the simulations generate a probability distribution that captures the variability in the final energy estimate. The parameters and their standard deviations used in the stored-heat calculation for Mount Ciremai are detailed in **Error! Reference source not found.**.

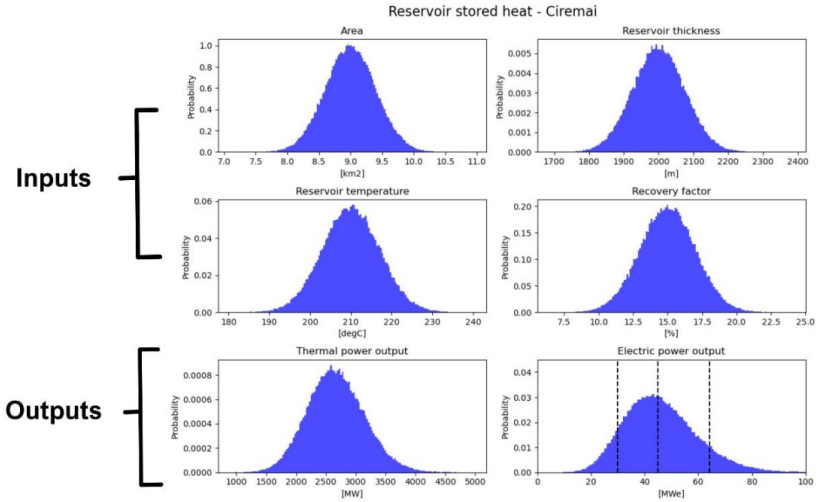

Figure 9: Monte Carlo Simulation Run Inputs and Outputs for Mount Ciremai Stored Heat Calculation

Table 1: Mean Parameters & Standard Deviations Used in Stored-Heat Calculation

Stored Heat Parameters	Units	Mean Values	Standard Deviations
Temperature[1]	°C	210	7
Porosity[2]	%	10	0.1
Reservoir coverage[3]	km^2	9	0.4
Reservoir thickness[4]	m	2000	75
Recovery factor[5]	%	15	0.02
Conversion efficiency[6]	%	12	-
Cut-off temperature[7]	°C	165	5
Rock density[8]	kg/m^3	2600	100
Rock specific heat[9]	kJ/kgK	1	0.05
Power plant operations year[10]	years	25	-

Note: (1) Based on geothermometer results for Cilengkrang hot spring
(2), (5), (6), (7) Based on Zarrouk & Simiyu (2013) for a medium enthalpy geothermal system
(3) (4) Derived from MT data of Mount Ciremai geothermal system
(8), (9), (10) Assumed

The Monte Carlo simulation results shown in **Error! Reference source not found.** predict a range of possible power outputs for the Mount Ciremai geothermal project over 25 years. The P90, P50, and P10 values are 29.8 MW, 44.8 MW, and 64.1 MW, respectively. While the method for estimating total heat seems reasonable, we need to be aware that there are limitations to the stored heat calculation since not all relevant factors are considered, and the Monte Carlo simulation itself cannot account for significant errors in assumptions about the resource size or recovery factor (Grant & Bixley, 2011).

7. 3D CONCEPTUAL MODEL CONSTRUCTION

Following the establishment of a robust conceptual model for the Mount Ciremai geothermal system, a crucial next step involves constructing a 3D digital conceptual model using specialized software called Leapfrog™, developed by Seequent Company. This 3D model was built upon the foundation of the existing conceptual model, which integrates various datasets including geology (stratigraphy, structures, or faults), geophysics (MT and others), geochemistry (resource fluid flow paths, potential temperatures, isothermal lines), and hydrology.

The primary purpose of the 3D digital conceptual model is to rigorously evaluate, validate, and potentially refine the conceptual model. Through this process, we can perform valuable follow-up analyses, such as sensitivity studies and data worth analysis (M. J. O'Sullivan & O'Sullivan, 2016). These analyses will serve to systematically improve the accuracy and resolution of the base conceptual model.

7.1 Geological Model

7.1.1 Topography Setup

Digital elevation data (X, Y, and Z coordinates) were sourced from publicly available datasets and subsequently imported into Leapfrog™ software to define the topography for the model. The model domain encompasses a 40 km radius centred on the summit of Mount Ciremai, the anticipated geothermal system centre. The selection of this extensive domain ensures a large enough volume is included to accommodate the large-scale convective system and its surrounding meteoric recharge zone within the reservoir model. The topography setup is illustrated in **Error! Reference source not found.**.

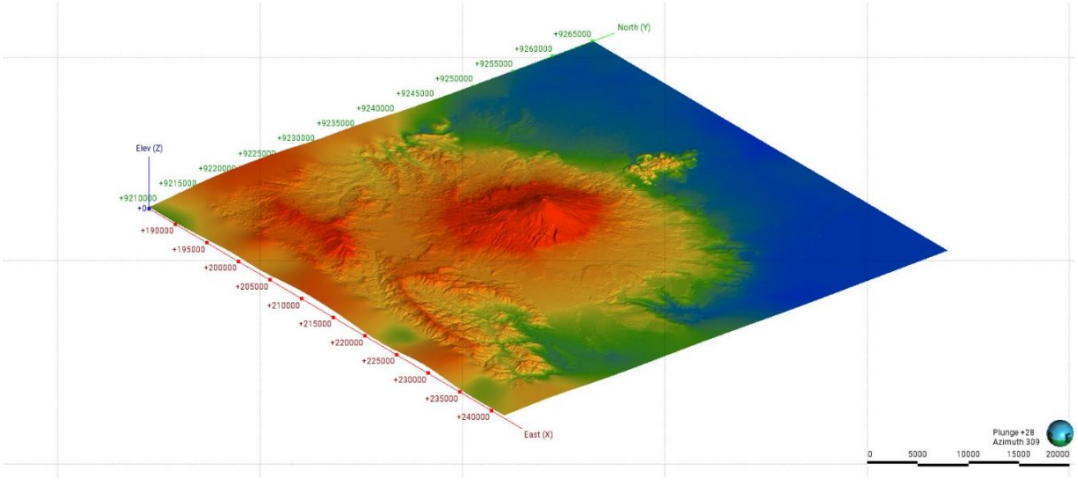

Figure 10: Topography set-up in Leapfrog™ for the 3D Digital Conceptual Model of Mount Ciremai Geothermal System

7.1.2 Stratigraphy Setup

The stratigraphical setup as an input for the Leapfrog™ model is based on the stratigraphical data from the literature review and is shown in **Error! Reference source not found.** below. It summarizes the rock units that were incorporated into the model, from the youngest to oldest rock formation.

Table 2: Stratigraphy Setup for 3D Digitized Conceptual Model Creation

Rock Formation	Abbreviation	Rock Code	Period	Epoch
Alluvium and Coastal Deposits	QA	-	Quartenary	Holocene
Young Volcanic eruptions	QYU	Y	Quartenary	Holocene
Old Volcanic eruptions	QVU	V	Quartenary	Holocene
Citalang Formation	TPC	C	Tertiary	Pliocene
Kaliwangi Formation	TPK	K	Tertiary	Pliocene
Ciherang Formation	TPCH	P	Tertiary	Pliocene
Halang Formation	TMH	H	Tertiary	Miocene
Cinambo Formation	TOMC	O	Tertiary	Oligocene

7.1.3 Lithology Setup

The lithological model for the Mount Ciremai geothermal system was constructed utilizing existing geological data. This included regional maps and cross-sections from Arjawinangun (Djuri, 2011) and Cirebon (Silitonga et al., 1996), which were integrated with the previously established topography data within Leapfrog™. Polylines were the primary tool used to define the digitized lithological model for Mount Ciremai. This process involved sequentially constructing the surface boundaries of each geological formation to create a 3D volume representation based on their chronological order of emplacement (Nagoro, 2023). A noteworthy observation during the Leapfrog™ lithological model construction was the "uplift" of the older rock formations (Cinambo Formation, rock code: TOMC and Halang Formation: rock code: TMH) located south of Mount Ciremai, extending laterally in a west-east direction. According to Rizal et al. (2019), the Cinambo Formation was originally deposited in the outer to middle part of a submarine fan environment, experiencing depositional mechanisms like saltation, suspension, and traction. This vertical displacement of the Cinambo sandstone formation is likely to be the result of ongoing geological processes (Rizal et al., 2019). These geological features were incorporated into the lithological model to reflect the characteristics of the formation and their potential influence on the geothermal system, as shown in **Error! Reference source not found.**.

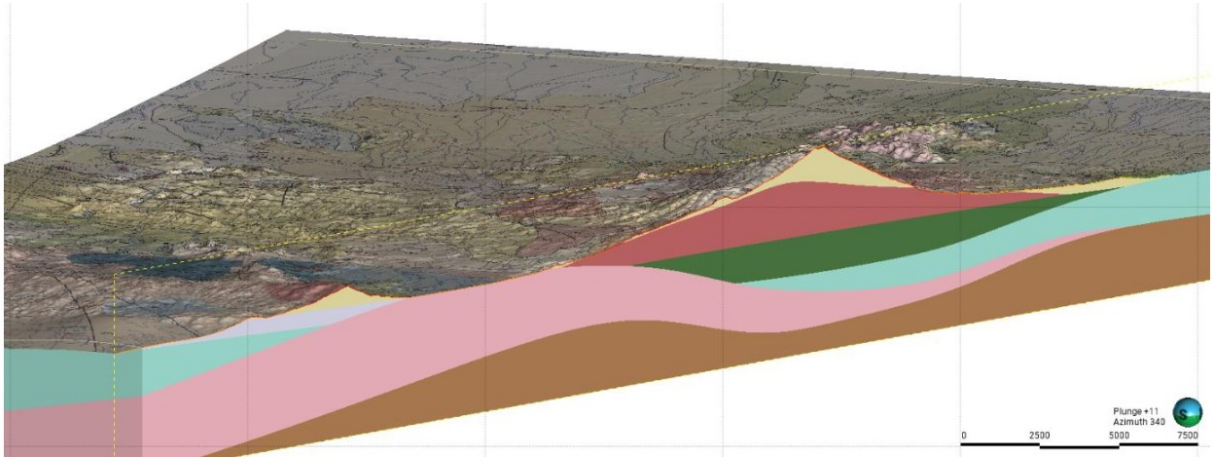

Figure 11: Lithological cross-section of Mount Ciremai area

7.1.4 Structural Interpretation

The 3D digital conceptual model incorporates the structural interpretation derived from two key literature sources including, Sulaesih et al. (2021), where the author employed LiDAR data overlaid on geological maps to map geological structures and Dewi et al. (2021) where she utilized Full Hyperspectral Data (FHD) and 2.5D modeling for structural mapping. The combined analysis led to the identification and digitization of a total of 14 faults into the Leapfrog™ software (**Error! Reference source not found.**). Detailed descriptions of these faults are provided in **Error! Reference source not found.**. Key faults and their roles in the 3D Digital Conceptual Model are:

- **B-Fault**: This major conduit structure plays a crucial role in fluid movement within the geothermal system. Notably, its intersection with the X-fault is believed to be responsible for the emergence of the Cilengkrang hot spring (surface manifestation).

- **"Pseudo" Boundaries**: Several faults act as partial barriers, influencing the direction of fluid flow. Caldera M and N faults, along with the D-fault, restrict flow towards the north and northwest. Similarly, the G-fault limits flow to the south and southeast, while the T and H faults act as boundaries for the northern region.

- **E-Fault**: Current interpretation suggests that the E-fault serves as the primary conduit for the outflow that feeds the Sangkanhurip and Ciniru hot springs.

The major conduit structure in the Mount Ciremai area is the B-fault, particularly where it intersects the X-fault, a fault that is responsible for the Cilengkrang hot springs (surface manifestation). A “pseudo” boundary is provided by the Caldera M and N and the D-fault, where they stop the flow to the north and northwestern area, and the G-fault acts as a barrier for the south to the southeastern area and T- and H-faults are a boundary for the northern area. The E-fault is currently interpreted as the fault that brings the outflow up to the Sangkanhurip and Ciniru hot springs.

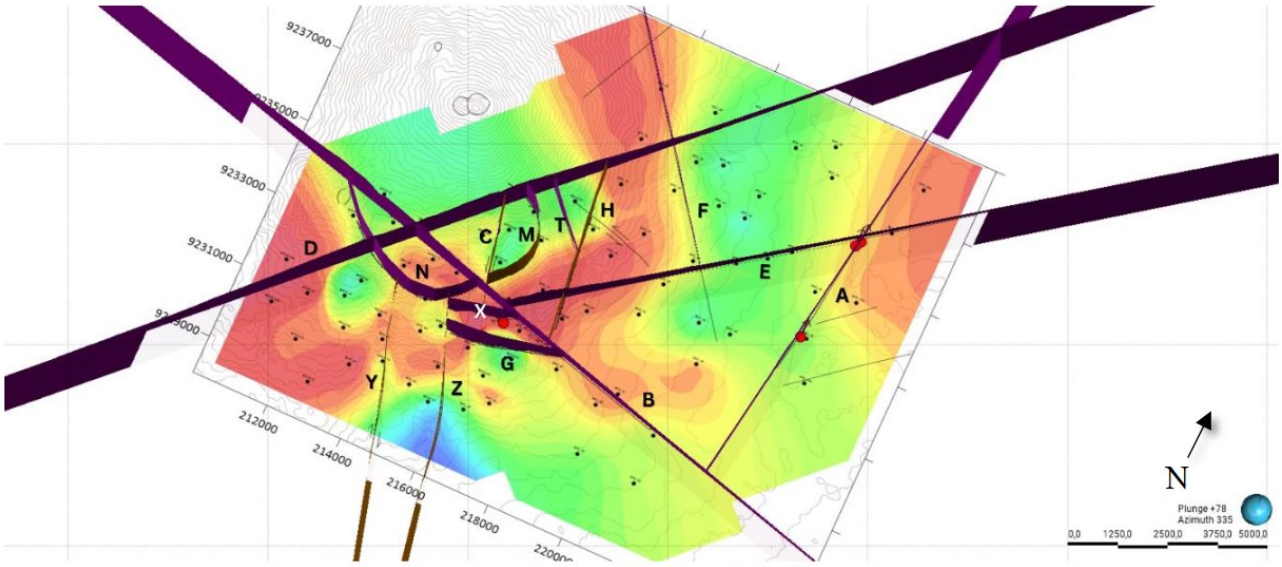

Figure 12: Digitization of Structures for the 3D-Geological Model

Table 3: Stratigraphy Setup for 3D Digitized Conceptual Model Creation

Faults Name	Orientation	Roles	Direction
A	N-S	Conduit	2
B	W-E	Conduit	1
C	NW-SE	Barrier	1
D	SW-NE	Barrier	1
E	SW-NE	Conduit	1
F	NW-SE	Barrier	2
G	SW-E	Barrier	1
H	N-S	Barrier	2
M	Caldera (opening to W)	Barrier	1
N	Caldera (open to N)	Barrier	1
T	NW-SE	Barrier	2
X	SW-E	Conduit	1
Y	NW-SE	Conduit	2
Z	NW-SE	Conduit	2

The construction of an accurate 3D digital conceptual model in Leapfrog™ software requires meticulous attention to detail during fault digitization. A crucial aspect is consideration of the relative ages of intersecting faults, as misinterpreting their chronological order can lead to errors in the structural framework of the model. Furthermore, accurately capturing the direction of each fault (across or along geological layers) is essential. This information plays a vital role in the calibration of the natural state model, as fault orientations influence fluid flow patterns within the geothermal system.

7.2 Alteration Model

The interpretation of the 3D clay cap for the Mount Ciremai geothermal system reveals two distinct dome-shaped features. The higher dome potentially correlates with the overlying surface manifestation – the Cilengkrang hot spring (as shown in **Error! Reference source not found.**). Conversely, the presence of the second dome without a corresponding surface manifestation suggests a potential upflow zone from the base of the system. This upflow zone may be a crucial factor in depicting the heat source location for the geothermal system, and further investigation is warranted to confirm its validity

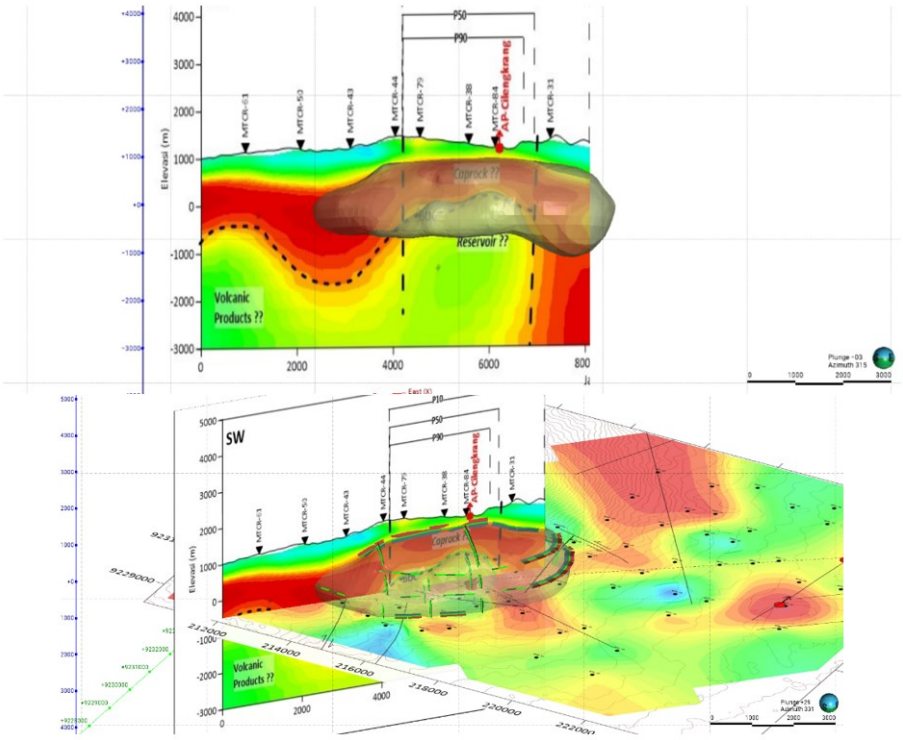

Figure 13: Clay cap zone that is constructed based on cross-sectional (Top) and plan-view (Bottom) MT data

7.3 Combined Model

By incorporating these diverse datasets (topography, lithology, stratigraphy, structures, and alteration zones), the 3D model provides a holistic representation of the Mount Ciremai geothermal system, serving as a valuable foundation for further analysis and resource assessment. The combined conceptual model is shown in **Error! Reference source not found.**.

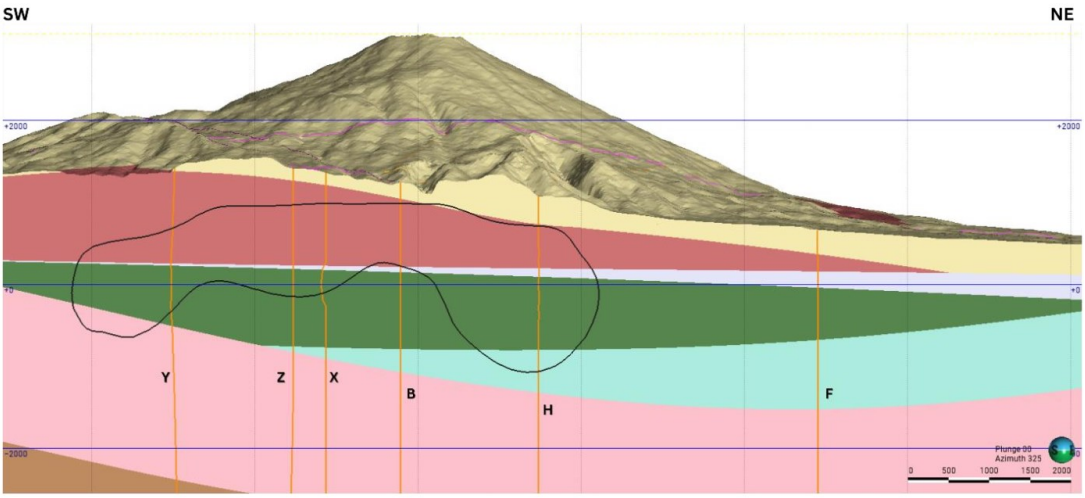

Figure 14: 3D Digital conceptual model (combined 3D model) of Mount Ciremai geothermal system, including rock unit, clay cap zone and faults

8. NUMERICAL RESERVOIR MODEL

Numerical simulation serves as a powerful tool for in-depth analysis of geothermal reservoirs. It is based on the numerical solution of the governing equations: mass and energy balance equations, Darcy's law, equation of states.

Numerical simulation allows us to: i) assess permeability structure, ii) estimate heat inputs, and iii) evaluate fluid inputs. By analyzing a "natural state model" first, we establish a baseline understanding of the system in its undisturbed state. This foundation is essential for simulating future behavior under various extraction scenarios. Ultimately, numerical simulation empowers us to optimize geothermal energy utilization for sustainable and cost-effective power generation (Suzuki et al., 2022).

8.1 Grid Setup

The generated model grid was based on the Leapfrog model and oriented 40° from the azimuth to align with the main fault strike, facilitating easier calibration of the numerical model. This grid covers an area of 12 km by 18.4 km, consisting of 39,089 blocks. The largest blocks measure 1000 m by 1000 m, and the vertical thicknesses of the layers range from 500 m at the base of the grid (Layer 53) to 100 m near the surface. In the zone of interest, a higher resolution was implemented, with a block size of 250 m by 250 m. The rock types of the blocks were automatically assigned to correspond with those in the Leapfrog model, a process seamlessly integrated using PyTOUGH (Croucher, 2011). **Error! Reference source not found.** shows the grid setup for this model.

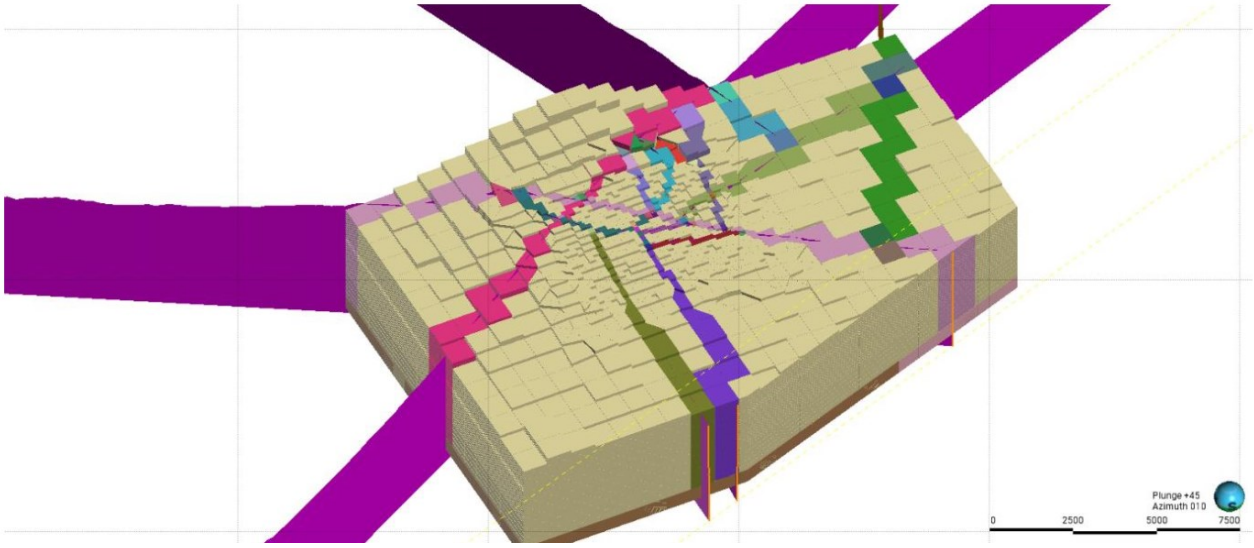

Figure 15: Grid Layout of Mount Ciremai 3D Conceptual Model imported to Leapfrog™. The area of interest around the centre of the system has a smaller grid of 250m x 250m

8.2 Boundary Condition

The allocation of boundary conditions is one of the most important aspects of model design (M. J. O'Sullivan & O'Sullivan, 2016). Therefore, we need to ensure that our numerical model can be run smoothly and effectively by setting the appropriate boundary conditions.

8.1.1 Top Boundary

For the top boundary, a dry atmospheric condition was assigned to the top surface of the model, with a pressure of 1 bar and a mean temperature of 15°C. The EOS3 equation-of-state module was employed to provide the thermophysical properties of a mixture of water and air, which were used as inputs for the mass and energy balance equations (Pruess et al., 1996).

8.2.2 Side Boundary

Following best practice, closed side boundaries were set up as far as possible from the zone of interest. However, to accurately represent the shallow groundwater flow from Mount Ciremai, deliverability (DELV) outflow conditions were implemented in the shallow formations of the side boundaries of the model. This approach ensures that the model aligns with the low elevation of the groundwater table, with a mean value of 490 m above sea level, found in the vicinity of the Mount Ciremai area (Irawan et al., 2009)

8.3.3 Base Boundary

The model incorporates two key components to represent the heat source driving the geothermal system. At the base, a uniform background heat flux of 80 mW/m² is applied, reflecting the natural geothermal gradient that increases temperature with depth. This provides a baseline heat input throughout the model.

To further simulate the specific deep upflows for this geothermal system, localized heat and mass inputs are applied. For this, we used 10 blocks located beneath the "Y" and "Z" faults, approximately located under the dome-shaped area of the clay cap. Here, hot water with an enthalpy of 1250 kJ/kg is injected at a total rate of 56 kg/s. This concentrated upflow represents the effect of deep convection adjacent to the deeper magmatic intrusion which is the heat source for the system. This provides a realistic representation of input of heat and mass to the geothermal system.

8.3 Rock Properties

In the numerical model, the assigned parameters represent the average properties within each volume. The configurable rock properties include density, porosity, permeability, heat conductivity, and specific heat of rock grains. Two crucial parameters representing the rock matrix properties are porosity and permeability. Porosity measures the average open pore space within the rock matrix, calculated as the percentage of space occupied by pores in a rock sample. Permeability measures the connectivity of these pores and significantly impacts the calibration of the numerical model.

In this model, rock parameters were directly assigned from the discretized zones of the combined model, categorized by lithology, fault zones, fault zone intersections, alteration, and heterogeneity, resulting in a large number (354) of different rock-type or classifications that need to be carefully and meticulously adjusted during the natural state model calibration process.

9. NATURAL STATE CALIBRATION AND SIMULATION

At the early stage of geothermal field development (exploration stage or pre-exploitation stage), only approximate simulations can be carried out because the amount of data available for quantitative calibration is limited (since no well data are available). However qualitative calibration can be carried out making sure that the numerical model is consistent with the conceptual model or else, as is often the case, discovering and fixing problems with the conceptual model (M. J. O'Sullivan & O'Sullivan, 2016). As the conceptual model is refined, the next step, resource potential estimation and uncertainty quantification result can be carried out, thus aiding the decision makers or investors to further develop the field.

9.1. Model Calibration

Model calibration is a critical step in reservoir modeling, where parameters like permeability and mass upflow are adjusted to match model outputs with real-world data (de Beer et al., 2023). This process can be challenging due to interactions between multiple parameters. While manual calibration is challenging, tools like TIM (Yeh et al., 2013) simplify the process. Key parameters adjusted in natural state modeling include rock permeability, resource mass and distribution, and resource enthalpy. Rock permeability is adjusted for rock types linked to geothermal activity, such as faults or structures that control fluid flow, with adjustments aligning with fault orientations and geological factors like overburden pressure, which reduces permeability at greater depths. Mass inputs and distribution were refined using geological and temperature data, while the initial enthalpy of the geothermal resource was set based on 3D geological data. In this study, an enthalpy of 1,250 kJ/kg was used, with the mass upflow distributed across 10 blocks.

This study employed manual calibration to improve the match between model results and observed data. Although automated methods exist (M. J. O'Sullivan & O'Sullivan, 2016), manual calibration offers advantages, such as greater control and the ability to apply expert knowledge of the system, ensuring informed decisions about parameter changes. Additionally, manual calibration helps researchers understand system dynamics and parameter sensitivity, such as how permeability impacts temperature distribution and the effect of the deep upflows. However, manual calibration can be time-consuming and subjective, suggesting that future work could explore hybrid methods combining manual and automated techniques for greater efficiency and accuracy.

To evaluate the geothermal system's energy potential, a comprehensive resource assessment was conducted, incorporating uncertainty quantification for more robust estimates. The natural state model was calibrated using two primary datasets: surface manifestation temperature data and estimated clay cap temperature. Surface manifestations provide valuable insights into system dynamics, helping to identify potential upflow and outflow zones. **Error! Reference source not found.** illustrates the calibrated natural state model of the Mount Ciremai geothermal system, visualized using the TIM application. It demonstrates the effectiveness of the calibration process in capturing the behaviour of the system.

9.2 Calibrated Natural State Model

Natural state calibration aligns closely with the conceptual model, matching surface manifestation temperatures and indicating a reservoir temperature of 210–230°C, consistent with geothermometer results. The heat source, probably distant from Mount Ciremai's magmatic pathway, heats fluids in volcanic-sedimentary rocks beneath the clay cap. These fluids emerge as the Cilengkrang hot springs (57°C), exhibiting a chloride-dominant composition with balanced sulfate and bicarbonate, reflecting magmatic Cl, H_2S, and CO_2 inputs. The fluid flows eastward to the Sangkanhurip and Ciniru chloride springs, typical of volcanic systems where outflows are distal to heat sources (Nicholson, 1993). The calibrated groundwater table, critical for resource assessment outcomes, aligns with field data and will be discussed further.

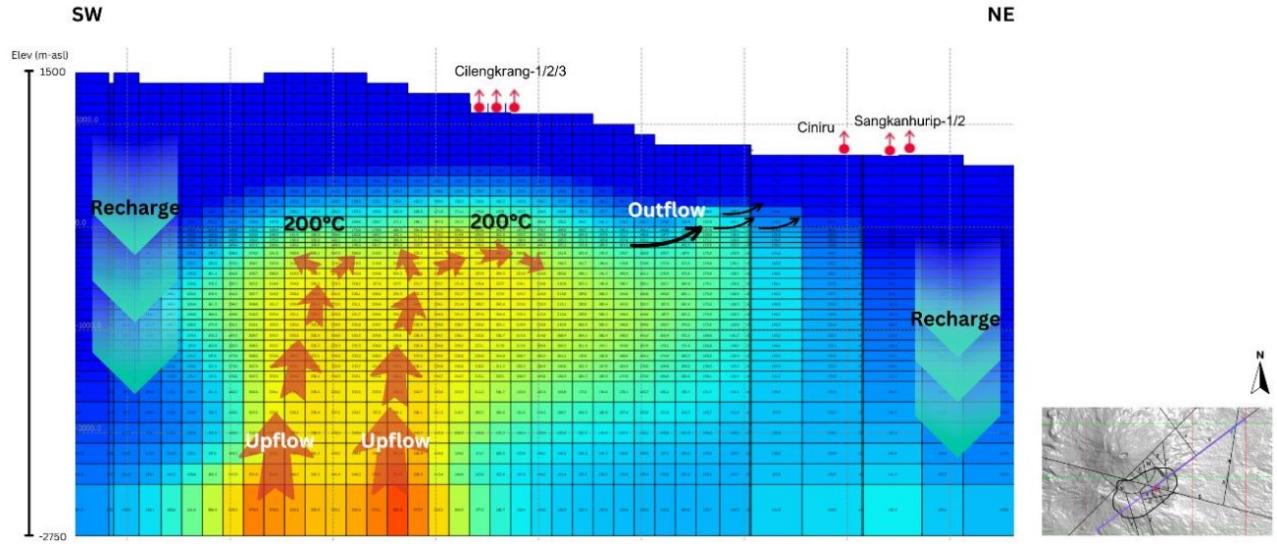

Figure 16: Mass flow and temperature distribution for Mount Ciremai Natural State Model

10. RESOURCE ASSESSMENT

Assessing the electricity generation potential of an undeveloped geothermal field is an essential first step, but it is fraught with challenges. The key obstacle lies in the limited availability of data. Gathering data from deep underground can be a prohibitively expensive and technically demanding endeavour. Even if some data can be acquired, there remains a significant degree of uncertainty regarding crucial subsurface features like the size and temperature distribution of the geothermal reservoir, as well as the permeability of the rock formations within it (Dekkers, et al., 2022). These risks and uncertainties make it difficult to precisely estimate the potential power output of the geothermal field, thus making the potential geothermal resources less attractive to investors.

While traditional methods like stored heat calculations offer a quick and easy approach, they often neglect the complex physical behaviour of geothermal fluids, leading to inaccurate estimations of power output. To address this limitation, Dekkers et al., (2022) introduced a new assessment method. This approach leverages numerical models coupled with probabilistic algorithms for a more robust evaluation.

The enabler for this lies in Waiwera, a high-performance reservoir simulation software developed by the University of Auckland and GNS Science (Croucher et al., 2020). The ability of Waiwera to run simulations in parallel on multiple cores significantly increases computational speed (M. O'Sullivan et al., 2021). Combined with the New Zealand eScience Infrastructur (NeSI) "Maui" supercomputer as the computing media, it allows for the creation and analysis of numerous models based on randomly sampled parameters. This step is crucial in addressing uncertainties within an undeveloped geothermal system.

This method is particularly suitable for a green field like Mount Ciremai geothermal field, where a more reliable initial assessment of the production scheme is desired. Building upon the results of the natural state model, information about rock types, properties, fault formations, and upflow zones serves as the foundation for these simulations. By analysing results from a large number of combinations of these parameters, researchers can carry out a robust assessment of the system. Figure 28 summarizes the framework of this new method.

10.1 Parameter Samples

The first step of the method involves sampling using the parameters used in the model by setting some uncertainty in the model parameters (Dekkers, Gravatt, Renaud, et al., 2022). For this case, the parameters are the total magnitude of the deep geothermal upflow, upflow location and distribution, and rock permeabilities. In this step, a sample model will include a random distribution of parameters that vary within a predefined reasonable range (Dekkers, Gravatt, Renaud, et al., 2022).

In total 1000 sample models were created and run to steady-state conditions, using random, reasonable values for the selected parameters. Of the 1000 sample models 995 ran to a converged steady state. These 995 models were further filtered by the temperature threshold of the clay cap as discussed in detail in the following section

10.2 Conditioning of Sample Models

Out of 995 initial sample models, this clay cap filtering process selected a set of 100 sample model that best meet the criteria for production scenarios. Sample #546 was ranked highest among the filtered set, while sample #31 was outside the 100 sample models selected and was excluded. **Error! Reference source not found.** utilizes Leapfrog™ software to visually compare the two samples, clearly showing how the selection method selects models which align properly with the conceptual model.

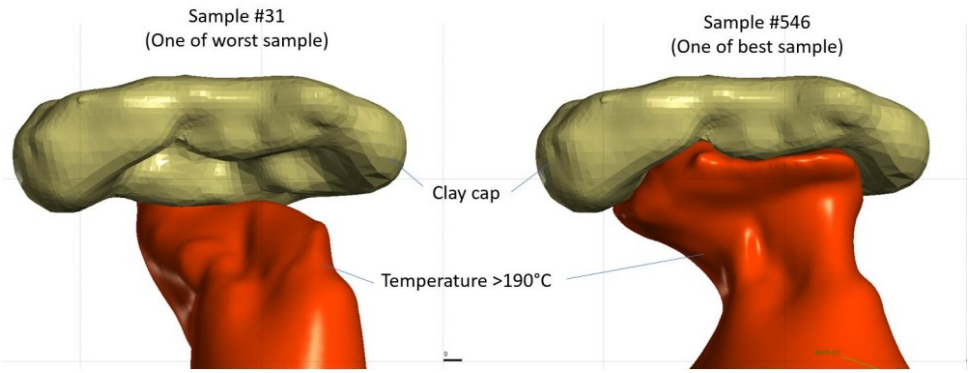

Figure 17: Result Comparison Between One of Best and One of Worst Sample Models for Clay Cap Conditioning

10.3 Production Scenario

Following the selection of acceptable steady-state sample models filtered by geophysical data, the next step of this method is to quantify and simulate the maximum potential production scenarios for each conditioned sample model using wellbore simulations to ensure accurate wellbore physics is included in the production estimates (Dekkers, Gravatt, Maclaren, et al., 2022). To achieve this, each steady-state model is used as the initial condition for a dedicated production simulation of a binary power plant with a 15% thermal to electrical power efficiency. The expected outcome is the prediction of the power output from the Mount Ciremai geothermal system, presented through probabilistic estimates (P10, P50, and P90).

10.4 Power Output

The initial resource assessment for the Mount Ciremai geothermal system presents a surprising result: based on current assumptions, the system's potential electricity generation capacity is estimated at least 1.1 MWe (P90) for about 25 years of operation, as illustrated in **Error! Reference source not found.**. This low output is a result of an important geological factor – the low groundwater table level in the Mount Ciremai area resulting in low reservoir pressures compared to the depth of the reservoir. The low reservoir pressures compared with the reservoir depth result in production wells that are unable to self-discharge and hence lead to a low power output estimate. This effect cannot be captured by the standard stored heat calculation described above other than through modifications of the recovery factor. This highlights the shortcomings of stored heat calculations as an accurate method for resource assessment. The production forecasts for the Mount Ciremai geothermal system that produced a resource assessment estimate of a minimum of 1.1 MWe (P90) over 25 years are shown in **Error! Reference source not found.**).

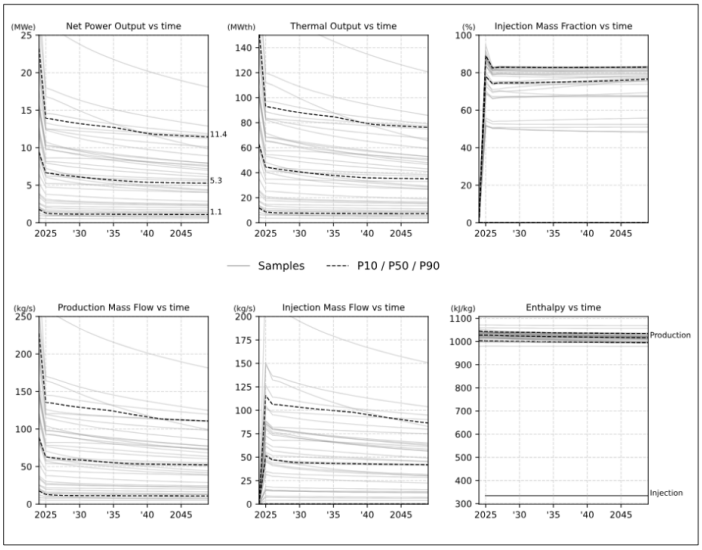

Figure 18: Illustration of the total resource potential of the Mt. Ciremai Geothermal system. From left to right and top to bottom, the diagrams display the estimated ranges for power output, steam flow rate, production mass flow, injection mass flow, and enthalpy

To assess the impact of low reservoir pressures compared to production well feed-zone depths, a second hypothetical scenario was created simulating production wells drilled from a 500 meters lower elevation via deviated drilling. This yielded P90/P50/P10 outputs of 29/38/55 MWe over 25 years, demonstrating a significantly improved discharge via an enhanced reservoir pressure compared to feed-zone pressure (Bernoulli equation). The results of the simulations are shown in **Error! Reference source not found.**. Simulating a 500-meter lower wellhead helps to assess impacts of low groundwater but remains theoretical for Mount Ciremai. To validate low groundwater effects, exploration drilling or shallow wells are essential. Artificial lift systems (pumps) could address low reservoir pressure, though cost-benefit analysis is required to evaluate feasibility.

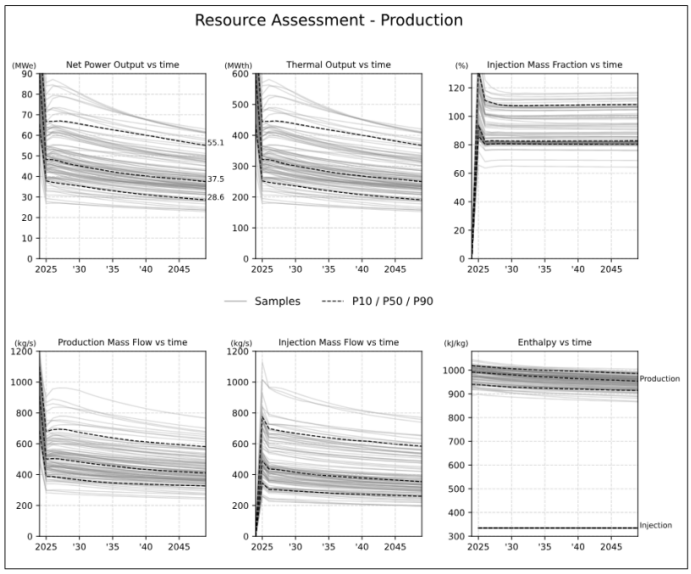

Figure 19: Optimistic results for Mount Ciremai resource assessment obtained by simulating an alternative scenario

11. CONCLUSION AND RECOMMENDATION

This study assessed the Mount Ciremai Geothermal System's potential for electricity generation using a multi-stage approach. A conceptual model was developed by integrating geological, geophysical, and geochemical (3G) data, representing a hydrothermal system where upflow beneath the clay cap emerges at the Cilengkrang hot springs and flows out at the Sangkanhurip and Ciniru hot springs. Numerical simulations were used to calibrate the natural state model and resulted in a total upflow of 56 kg/s distributed across 10 blocks (enthalpy: 1,250 kJ/kg). The model provided insights into fluid flow, temperature distribution, and reservoir characteristics. Groundwater level data from the literature was also incorporated to enhance accuracy.

Uncertainty quantification was applied to generate a resource assessment using realistic production scenarios. Using high-performance computing, approximately 1,000 models were created and filtered, resulting in 100 acceptable models. These were simulated for 25-year production from a binary system with 15% thermal efficiency. Initial estimates showed limited outputs (1.1/5.3/11.4 MWe), significantly lower than the stored heat calculation (44.8 MWe), due to low groundwater levels resulting in low reservoir pressure. A deviated well scenario with wells located at a lower elevation improved outputs to 29/38/55 MWe, highlighting two key findings:

a. **The importance of numerical modelling with uncertainty in estimating resource potential:** Numerical modelling with uncertainty is critical for estimating geothermal resource potential, especially with limited data. This study highlights its ability to provide more accurate estimates compared to traditional methods like stored heat calculations at the pre-development stage. Recent advancements enable testing multiple numerical models, improving accuracy and supporting informed decisions for geothermal development.

b. **The importance of groundwater level data in the geothermal system pre-development stage:** Groundwater elevation can critically influence reservoir pressure. XU Hao et al., (2008) demonstrated that lower groundwater levels reduce hydrostatic pressure, disrupting fluid flow and energy extraction. Thus, groundwater level data should be collected alongside geological, geochemical, and geophysical datasets to enhance numerical modelling accuracy and improve geothermal potential assessments.

Future efforts should prioritise collecting additional data, particularly comprehensive magneto-telluric (MT) surveys, to enhance understanding of the Mount Ciremai system. Integration of new datasets (e.g., MT, exploration well pressure/temperature, flow tests) will improve the robustness of numerical models, supporting informed development decisions.

Further hydrogeological studies are recommended to clarify groundwater's role in reservoir performance. Hydrogeological data should also be prioritised in early-stage assessments for other geothermal prospects.

ACKNOWLEDGEMENTS

The authors would like to acknowledge the Directorate General of New, Renewable Energy and Energy Conservation (EBTKE) and the Geological Agency of the Ministry of Energy and Mineral Resources of Indonesia for providing the data related to the Mount Ciremai Geothermal Field. The authors also thank Seequent for providing a license for the Leapfrog Energy software, which was essential to this research.

REFERENCES

Boseley, C., Cumming, W., Urzúa-Monsalve, L., Powell, T., Grant, M., Geoscience, C., Runciman, D., & Boseley, C. (2010). *A Resource Conceptual Model for the Ngatamariki Geothermal Field Based on Recent Exploration Well Drilling and 3D MT Resistivity Imaging*. World Geothermal Congress 2010, Bali, Indonesia.

Croucher, A. (2011, November 21). PYTOUGH: A PYTHON SCRIPTING LIBRARY FOR AUTOMATING TOUGH2 SIMULATIONS. *New Zealand*. New Zealand Geothermal Workshop, Auckland, New Zealand.

Croucher, A., O'Sullivan, M., O'Sullivan, J., Yeh, A., Burnell, J., & Kissling, W. (2020). Waiwera: A parallel open-source geothermal flow simulator. *Computers & Geosciences*, *141*, 104529. https://doi.org/10.1016/j.cageo.2020.104529

Cumming, W. (2009, February 9). *GEOTHERMAL RESOURCE CONCEPTUAL MODELS USING SURFACE EXPLORATION DATA*. 34th Workshop on Geothermal Reservoir Engineering, Stanford, California. https://www.researchgate.net/publication/228643656_Geothermal_resource_conceptual_models_using_surface_exploration_data

Dekkers, K., Gravatt, M., Maclaren, O. J., Nicholson, R., Nugraha, R., O'Sullivan, M., Popineau, J., Riffault, J., & O'Sullivan, J. (2022, February 7). *Resource Assessment: Estimating the Potential of a Geothermal Reservoir*. 47th Workshop on Geothermal Reservoir Engineering, Stanford, California. https://www.semanticscholar.org/paper/Resource-Assessment%3A-Estimating-the-Potential-of-a-Dekkers-Gravatt/98bff9f424bd65870639c689f1d7eb1e60bdd715?utm_source=chatgpt.com

Dekkers, K., Gravatt, M., Renaud, T., Beer, A., Power, A., Maclaren, O., Nicholson, R., O'Sullivan, M., Riffault, J., & O'Sullivan, J. (2022, November 6). *Resource Assessment: Estimating the Potential of an African Rift Geothermal Reservoir*.

Dewi, R., Widodo, S., & Taryana, D. (2021). Survei Rinci Gaya Berat Daerah Panas Bumi Ciremai, Kabupaten Kuningan, Provinsi Jawa Barat. *PROSIDING HASIL KEGIATAN PUSAT SUMBER DAYA MINERAL BATUBARA DAN PANAS BUMI TAHUN ANGGARAN 2021. KEMENTERIAN ENERGI DAN SUMBER DAYA MINERAL*, *3*, 221–230. https://geologi.esdm.go.id/storage/publikasi/GPFrrXdlaOTkrU7DYmwIY4KGKtbNxgZ7pm3MJkat.pdf

Djuri. (2011). *Peta Geologi Lembar Arjawinangun, Jawa.* (Edisi 3) [Map]. Pusat Penelitian dan Pengembangan Geologi.

Glassley, W. E. (2010). *Geothermal Energy: Renewable Energy and the Environment*. CRC Press. https://doi.org/10.1201/EBK1420075700

Grant, M. A., & Bixley, P. F. (Eds.). (2011). Geothermal Reservoir Engineering. In *Geothermal Reservoir Engineering (Second Edition)* (p. iii). Academic Press. https://doi.org/10.1016/B978-0-12-383880-3.10022-8

Irawan, D. E., Puradimaja, D. J., Notosiswoyo, S., & Soemintadiredja, P. (2009). Hydrogeochemistry of volcanic hydrogeology based on cluster analysis of Mount Ciremai, West Java, Indonesia. *Journal of Hydrology*, *376*(1), 221–234. https://doi.org/10.1016/j.jhydrol.2009.07.033

Kusnadi, D., Nirmala, W., & Nahar, K. (2021). Survei Rinci Geokimia (PERTAGASTECH) Daerah Panas Bumi Gunung Ciremai, Kabupaten Kuningan, Provinsi Jawa Barat. *PROSIDING HASIL KEGIATAN PUSAT SUMBER DAYA MINERAL BATUBARA DAN PANAS BUMI TAHUN ANGGARAN 2021. KEMENTERIAN ENERGI DAN SUMBER DAYA MINERAL*, *3*, 209–219. https://geologi.esdm.go.id/storage/publikasi/GPFrrXdlaOTkrU7DYmwIY4KGKtbNxgZ7pm3MJkat.pdf

Nagoro, B. B. R. (2023, February 6). *Quantifying Geothermal Resource Potential and Uncertainty Analysis using a Natural State Model of Kotamobagu Geothermal Field in North Sulawesi*. 45th New Zealand Geothermal Workshop, Auckland, New Zealand.

Nicholson, K. (1993). *Geothermal Fluids: Chemistry and Exploration Techniques*. Springer. https://doi.org/10.1007/978-3-642-77844-5

O'Sullivan, M. J., & O'Sullivan, J. P. (2016). 7—Reservoir modeling and simulation for geothermal resource characterization and evaluation. In R. DiPippo (Ed.), *Geothermal Power Generation* (pp. 165–199). Woodhead Publishing. https://doi.org/10.1016/B978-0-08-100337-4.00007-3

O'Sullivan, M., Renaud, T., Gravatt, M., Riffault, J., Popineau, J., O'Sullivan, J., Ruiz, N., & Sophy, M. (2021, November 23). *An updated numerical model of the Ohaaki geothermal field*. 43rd New Zealand Geothermal Workshop, Wellington, New Zealand.

Pruess, K., Oldenburg, C., & Moridis, G. (1996). *TOUGH2 USER'S GUIDE, VERSION 2.0* (LBNL-43134). Earth Sciences Division, Lawrence Berkeley National Laboratory. https://tough.lbl.gov/assets/files/02/documentation/TOUGH2_V2.0_Users_Guide.pdf

Rizal, Y., Santoso, W. D., Djanuismawan, S., Rudyawan, A., & Nurfarhan, A. A. (2019). Sedimentation Study of Sandstone Turbidite Sequence of Cinambo Formation in Maja Area, Majalengka, West Jawa – Indonesia. *Earth Sciences*, *8*(3), Article 3. https://doi.org/10.11648/j.earth.20190803.17

Silitonga, P. H., Masria, M., & Suwarna, N. (1996). *Peta Geologi Lembar Cirebon, Jawa.* (1st Edition) [Map]. Pusat Penelitian dan Pengembangan Geologi.

Sukaesih, Permana, L. A., & Rezki, Y. (2021). SURVEI RINCI GEOLOGI DAERAH PANAS BUMI GUNUNG CIREMAI KABUPATEN KUNINGAN, PROVINSI JAWA BARAT. *PROSIDING HASIL KEGIATAN PUSAT SUMBER DAYA MINERAL BATUBARA DAN PANAS BUMI TAHUN ANGGARAN 2021. KEMENTERIAN ENERGI DAN SUMBER DAYA MINERAL*, *3*, 193–208. https://geologi.esdm.go.id/storage/publikasi/GPFrrXdlaOTkrU7DYmwIY4KGKtbNxgZ7pm3MJkat.pdf

Suzuki, A., Fukui, K., Onodera, S., Ishizaki, J., & Hashida, T. (2022). Data-Driven Geothermal Reservoir Modeling: Estimating Permeability Distributions by Machine Learning. *Geosciences*, *12*(3), Article 3. https://doi.org/10.3390/geosciences12030130

Takodama, I., Wahyuningsih, R., & Sugianto, A. (2021). Survei Rinci Magnetotelurik dan Time-Domain Electromagnetic Daerah Panas Bumi Gunung Ciremai, Kabupaten Kuningan, Provinsi Jawa Barat. *PROSIDING HASIL KEGIATAN PUSAT SUMBER DAYA MINERAL BATUBARA DAN PANAS BUMI TAHUN ANGGARAN 2021. KEMENTERIAN ENERGI DAN SUMBER DAYA MINERAL*, *3*, 193–208. https://geologi.esdm.go.id/storage/publikasi/GPFrrXdlaOTkrU7DYmwIY4KGKtbNxgZ7pm3MJkat.pdf

XU Hao, TANG Da-zhen, ZHANG Jun-feng, & YIN Wei. (2008). Mechanism of water table effecting reservoir pressure. *COAL GEOLOGY & EXPLORATION*, *38*(5), 31-33,37.

Zarrouk, S., & Simiyu, F. (2013). *A REVIEW OF GEOTHERMAL RESOURCE ESTIMATION METHODOLOGY*. 142–153.